ELSEVIER

NUTRITION

Nutrition 25 (2009) 581–589

www.nutritionjrnl.com

Basic nutritional investigation

Effects of calcium sources and soluble silicate on bone metabolism and the related gene expression in mice

Fusako Maehira, Ph.D.[a,*], Ikuko Miyagi, B.S.[a], and Yukinori Eguchi, Ph.D.[b]

[a] *Laboratory of Biometabolic Chemistry, School of Health Sciences, Faculty of Medicine, University of the Ryukyus, Nishihara, Okinawa, Japan*
[b] *Research Laboratory Center, Faculty of Medicine, University of the Ryukyus, Nishihara, Okinawa, Japan*

Manuscript received August 20, 2008; accepted October 29, 2008.

Abstract

Objective: The effects of five calcium (Ca) sources were compared for bone biochemical and mechanical properties and the related gene expression using mice, from the viewpoint of their soluble silicon (Si) content.

Methods: Weanling male mice were fed diets containing 1% Ca supplemented with $CaCO_3$ as the control (CT), coral sand (CS), fossil stony coral (FSC), fish bone (FC) and eggshell (EC) powders, and 50 ppm of Si in the CT diet for 6 mo. The mRNA expressions related to bone remodeling were quantified by real-time polymerase chain reaction.

Results: Soluble Si content was 9.83, 7.17, 2.48, 0.29, and 0.20 ppm for the CS, FC, FSC, EC, and Ca-deficient basal diets, respectively. Si, CS, and FSC, in order, significantly increased dry and ash weights, Ca and hydroxyproline contents, and alkaline phosphatase and decreased tartrate-resistant acid phosphatase and urinary excretion of hydroxyproline compared with the CT group. Si significantly increased and FC decreased femoral strength and stiffness. In the mRNA expression related to osteoblastogenesis, Si and CS significantly increased runt-related transcription factor 2. Si, CS, and FSC, in order, significantly decreased and FC and EC increased peroxisome proliferator-activated receptor-γ. In the mRNA expression related to osteoclastogenesis, Si and CS significantly increased and FC and EC decreased the osteoprotegerin/receptor activator of nuclear factor-κB ligand ratio, whereas Si and CS decreased transforming growth factor-β.

Conclusion: The results indicated that soluble silicate and CS, with the highest Si content among Ca sources, improved bone biochemical and mechanical properties through stimulation of gene expression related to osteoblastogenesis and suppression of that related to osteoclastogenesis.

Keywords: Soluble silicate; Coral sand; Bone metabolism; Mechanical properties; Gene expression

Introduction

Osteoporosis is a prevalent condition that may exist as a silent form with aging, and is characterized by low bone mass and microarchitectural deterioration of bone tissues with a consequent increase of bone fragility and susceptibility to fracture [1]. Unfortunately, although millions of people worldwide are afflicted by debilitating bone loss, few treatments halt or reverse its progression. According to the National Osteoporosis Foundation, osteoporosis is a major public health threat, having medical and economic impacts in the United States: 10 million individuals in the United States alone have osteoporosis, and almost 34 million more have low bone mass, being at increased risk for osteoporosis [2]. This multifactorial pathology involves genetic and environmental factors. People with genetic risk factors are considered more susceptible to lifestyle factors, including exercise and nutritional considerations concerning calcium (Ca), vitamin D, magnesium, and other trace minerals.

Calcium is the most common mineral in the human body and approximately 99% of total Ca is distributed in the bones, with the remaining 1% in the extracellular fluid. To achieve a suitable bone mass, which is an important determinant of bone strength to prevent involuntary fracture risk, dietary intake and urinary excretion of Ca are the most

* Corresponding author. Tel./fax: +81-98-895-1277.
E-mail address: fmaehira@med.u-ryukyu.ac.jp (F. Maehira).

0899-9007/09/$ – see front matter © 2009 Published by Elsevier Inc.
doi:10.1016/j.nut.2008.10.023

important factors. Such Ca homeostasis in the body is regulated by circulating hormones and rapid exchange between blood and bone Ca takes place at all bone surfaces in contact with blood by three essential mechanisms (apposition/resorption, rapid exchange, and diffuse exchange) determining the uptake and loss of bone-seeking elements [3]. There is accumulated evidence that Ca and other cations may regulate bone remodeling interaction with cell surface calcium-sensing receptors (CaRs) located in the plasma membranes of osteoblasts and osteoclasts [4,5]. CaR is thought to regulate numerous cellular processes through the intracellular signaling pathway under normal and pathologic conditions: proliferation, differentiation, apoptosis, and gene expressions associated with bone remodeling [4]. Potential CaR agonists and modulators include phosphate anion [6] in addition to calcium and other cations such as Mg^{2+} [4], Sr^{2+} [3,7], and Al^{3+} [8]; therefore, mobilization and deposition of Ca into the bone matrix involve several mineral interactions. Trace mineral involvement in bone metabolism, particularly copper, manganese, and zinc, have been extensively studied in animals [9]. The essentiality of silicon (Si) is demonstrated in chicks and rats through effects on growth and skeletal development [10,11]: abnormalities involving articular cartilage and connective tissue occur in chicks on Si-deficient diets. Si is involved in an early stage of bone calcification: Si has been uniquely localized in an active growth area in young bone of mice and rats [12]. It was found that in the fibrous layer of the periosteum Ca and Si values are invariably low, whereas in the adjacent osteoid layer Si-rich sites appear, containing up to 25 times as much Si and 9 times as much Ca as in the fibrous layer. The Si content in the sites decreases to the original extremely low value as Ca approaches the proportions in bone apatite. In other words, the more "mature" the bone mineral, the smaller the amount of measurable Si. Si in serum and tissues is present almost entirely as free soluble monosilicic acid, which is freely diffusible across the cellular membrane [13,14], resulting in rapid renal clearance with half-lives of 2.7 h for a fast component and 11.3 h for a slower component, that account for 90% and 10% of the absorbed dose, respectively [15,16]. The latter slower component may represent an intracellular fraction that may be involved in physiologic function [17]. Such rapid clearance of inorganic Si may be a potential benefit of long-term intake without excessive retention and accumulation in the body. We recently studied the effects of soluble Si as sodium metasilicate and deep sea water from a 612-m depth, containing about 30 times more soluble Si than surface sea water from which NaCl was eliminated, in comparison with tap water and surface sea water in the cell culture and in a mouse experiment [18]. The results indicated that soluble Si and deep sea water as natural material stimulated cell growth, with the highest activities of alkaline phosphatase (ALP) in osteoblasts and tartrate-resistant acid phosphatase (TRACP) in osteoclasts, enhanced $^{45}CaCl_2$ uptake in those cells in comparison with the medium control in the cell culture, and promoted bone metabolic turnover in favor of bone formation through stimulation of the related mRNA expression in animal experiments. In the present study, the effects of five Ca sources were compared on biochemical and mechanical properties of bone and the related gene expression using the control strain of senescence-accelerated mice (SAMR1), from the viewpoint of their soluble Si content. Soluble Si content was highest in coral sand (CS) among the five Ca sources tested: CS, fossil stony coral (FSC), fish (FC) and eggshell (EC) powders, and Ca carbonate (CT) as the control.

Materials and methods

Definition of corals used in this study and measurement of soluble Si

Corals are classified into reef-building (hermatypic) corals, characterized by symbiotic algae, Zooxanthella, which support their survival and calcification for building reefs, and non–reef-building (ahermatypic) corals without a symbiont. Hermatypic corals are found in shallow seas of a maximum 150 m in depth.

Coral sand

Coral reefs are destroyed by waves over many (approximately hundreds) years and are deposited on the sea floor in particle sizes by sieving with the water current. CS composes a major part of coral-reef deposit and is mainly derived from biological origin, such as pieces of calcareous algae, a shellfish, foraminifera, echinoderm, and from nonbiological carbonate salts. Collections of CS are strictly regulated by the Japanese government and Okinawa prefecture. CS smaller than approximately 1 cm is collected from the sea floor at 55–60 m in depth in the designated sea region by pumping up using a sand pump with a mesh filter, and large CS is returned to the sea. Crude CS smaller than approximately 2 mm is disinfected at 120–200°C and ground into a fine powder to smaller than 22 μm, which will dissolve in acidic solution or gastric juice.

Fossil stony coral

Earth crush fluctuations by tectonic subsidence and upheaval bury reef-building corals living in the shallow sea floor and create oceanic islands or mountains where corals become FSC and eventually coral limestone over approximately 1 million years. Although CS and FSC originate from hermatypic corals, their mineral constituents are different due to the method and period of weathering by wind and water.

Measurement of soluble Si

Acid-washed polyethylene vessels were used in all procedures to avoid Si contamination released from glassware, and double-distilled water was used. Soluble Si was extracted from 2.0 g of sample diets or no sample with 20.0

mL of double-distilled water in a 50-mL centrifuge tube by mixing for 1 min on a vortex followed by shaking for 24 h at room temperature. After centrifugation of the extracts at 15 000 rpm for 30 min at 4°C, the soluble fraction was filtrated through a 0.22-μm sterile filter. The filtrates and sodium hexafluorosilicate (Na_2SiF_6) as a standard were analyzed in duplicate by the molybdate method. Bioavailable soluble silicate, monosilicic acid, reacts with molybdate reagent to produce a yellow color, whereas amorphous silica or polysilicic acid does not react with this reagent [19]. Soluble Si content was 9.83, 7.17, 2.48, 0.29, and 0.20 ppm for the CS, FC, FSC, EC, and Ca-deficient purified diets, respectively.

Animal experiments

The control strain of senescence-accelerated mouse, SAMR1, was provided by the Council for SAM Research, Kyoto University (Kyoto, Japan), where these mouse strains were developed. The experimental protocols of this study were approved by our institutional animal studies committee. Weanling male SAMR1 1 mo of age were divided into six groups of 10 each. Animals were maintained for 6 mo on an ad libitum semisolid diet of 34% tap water and 66% powder diet (Table 1) containing 1% Ca supplemented with $CaCO_3$ as the CT, CS, FSC, FC, and EC powders in Ca-deficient purified diet (Oriental Yeast, Tokyo, Japan), and 50 ppm of Si supplementation to the CT diet, which had an Si dose lower than the range of 100–500 ppm, as used in previous studies, without toxic actions [10–13,18]. At the end of the experiments, urine was collected over a 24-h period with our handmade urine traps and was used to measure the urinary contents of hydroxyproline (OHPro) [20]. Urinary OHPro was corrected for creatinine excreted in urine. Supernatants from homogenates of the right tibia, after removal of its marrow, were assayed in duplicate for ALP activity at pH 10.5 for 15 min and TRACP activity at pH 4.9 for 60 min with absorbance at 500 nm by the Kind-King method and the activities were expressed as King-Armstrong Unit (K-A U) per milligram of protein. Mechanical tests were performed on the left femur, after cleaning soft tissue, in 3-point bending using an EZ Test-100N (Shimazu, Kyoto, Japan) [21]. After mechanical tests, the wet, dry (100°C, 24 h), and ash (500–550°C, 24 h) weights of the left femur were measured, followed by Ca by the o-Cresolphthalein complex method and phosphorus by the phosphomolybdenum blue method [22] after dissolving ash in acid, respectively. Acid digests of the right femur after removal of its marrow were used to measure OHPro and hexosamines (Hex). Collagen content was determined as OHPro by oxidizing OHPro into pyrrole followed by coupling with *p*-dimethyl-amino-benzaldehyde [23]. Glycosaminoglycan was analyzed as Hex [24] by a modification [25] of the Elson-Morgan method.

Table 1
Mineral composition of diet 100 g

Groups	CT	Si	CS	FCS	FC	EC
Major Ca salts	$CaCO_3$	$CaCO_3$	$CaCO_3$	$CaCO_3$	$CaPO_4$	$CaCO_3$
Ca (g)	1.11	1.11	1.11	1.11	1.11	1.11
Mg	0.23	0.23	0.30	0.25	0.25	0.23
Na	0.23	0.23	0.24	0.23	0.23	0.23
K	0.85	0.85	0.84	0.85	0.84	0.84
P	0.81	0.81	0.81	0.81	1.35	0.81
Fe (mg)	32.00	32.00	32.21	32.30	31.07	31.07
Zn	4.96	4.96	4.96	5.03	4.95	4.95
Cu	0.73	0.73	0.73	0.73	0.73	0.73
Mn	5.32	5.32	5.67	5.40	5.16	5.16
Si (μg)	18.9	5000	48.3	26.0	39.8	19.7

Ca, calcium; CS, coral sand; CT, calcium carbonate (control); Cu, copper; EC, eggshell; FC, fish bone; Fe, iron; FSC, fossil stony coral; K, potassium; Mg, magnesium; Mn, manganese; Na, sodium; P, phosphorus; Si, silicon; Zn, zinc

RNA isolation and gene expression analysis

Total RNA was isolated from bone marrow of the right femora and tibiae at the end of animal experiments using a NucleoSpin RNA II kit (Macherey-Nagel, Düren, Germany). Two micrograms of RNA was used for cDNA synthesis by reverse transcription with an Omniscript RT kit (Qiagen, Germantown, MD, USA). Quantitative real-time polymerase chain reaction (PCR) was performed using the Mx3000P real-time PCR system (Stratagene, La Jolla, CA, USA) and fluorescent dye SYBR Green (Brilliant SYBR Green QPCR Master Mix, Stratagene) to detect a double-strand DNA amplicon. The mRNA expression of genes related to osteoblastogenesis and osteoclastogenesis such as runt-related transcription factor 2 (Runx2), bone morphogenic protein-2 (BMP-2), interleukin-11 (IL-11), type I procollagen (COL1A1), peroxisome proliferator-activated receptor-γ (PPAR-γ), transforming growth factor-β (TGF-β), osteoprotegerin (OPG), and receptor activator of nuclear factor-κB ligand (RANKL) was analyzed using the pairs of primers summarized in Table 2. All real-time PCR reactions contained first-strand cDNA corresponding to 1–10 ng of RNA. The PCR protocol included the following cycling conditions: 95°C denaturation for 10 min, then 45 cycles of 95°C denaturation for 30 s followed by 60°C annealing for 1 min, and 72°C extension for 30 s. The fluorescent amplicon was mostly detected at the end of the 60°C annealing period. PCR products were subjected to melting curve analysis and quantified with Mx3000*P* 1.20c (Stratagene). PCR results were normalized to the expression of glyceraldehydes-3-phosphate dehydrogenase (GAPDH) in the same samples. Triplicate analyses were performed for each sample.

Statistical analysis

Experimental results are reported as the mean ± SD of an average from duplicate analyses for the animal specimens, unless otherwise indicated. Statistical analyses were performed by comparing mean values by using one-way analysis of variance with the SAS program (SAS Institute,

Table 2
Primer sequences for real-time polymerase chain reaction

Target gene	Probe	Primers	Product size (bp)
GAPDH	F	5′-AACGACCCCTTCATTGAC-3′	191
	R	5′-TCCACCACATACTCAGCAC-3′	
Runx2	F	5′-GCTTCATTCGCCTCACAAACA-3′	68
	R	5′-TGCAGTCTTCCTGGAGAAAGTT-3′	
BMP-2	F	5′-CTTCTAGTGTTGCTGCTTCC-3′	143
	R	5′-CTCAACTCAAATTCGCTGAG-3′	
IL-11	F	5′-CTCTTGATGTCTCGCCTG-3′	112
	R	5′-CTAGGATGGCATGAGCTG-3′	
COL1A1	F	5′-GAGATGATGGGGAAGCTG-3′	137
	R	5′-ACCATCCAAACCACTGAAG-3′	
PPAR-γ	F	5′-CGAGCCCTGGCAAAGCATTTGTAT	90
	R	5′-TGTCTTTCCTGTCAAGATCGCCCT	
TGF-β1	F	5′-GCCCTGGATACCAACTATTGCT-3′	161
	R	5′-AGGCTCCAAATATAGGGGCAGG-3′	
OPG	F	5′-GCACCTACCTAAAACAGCAC-3′	113
	R	5′-GCTGCAATACACACACTCAT-3′	
RANKL	F	5′-GCTCTGTTCCTGTACTTTCG-3′	100
	R	5′-CTGCGTTTTCATGGAGTC-3′	

BMP-2, bone morphogenic protein-2; COL1A1, type I procollagen; F, forward; GAPDH, glyceraldehydes-3-phosphate dehydrogenase; IL-11, interleukin-11; OPG, osteoprotegerin; PPAR-γ, peroxisome proliferator-activated receptor-γ; R, reverse; RANKL, receptor activator of nuclear factor-κB ligand; Runx2, runt-related transcription factor 2; TGF-β1, transforming growth factor-β1

Cary, NC, USA) and individual differences between groups were assessed using Duncan's multiple range test, in which the means with different letters are significantly different at $P < 0.05$.

Results

Effects on biochemical and mechanical properties of bone

All animals appeared healthy during the 6 mo of the study period and there was no significant difference in weight gains among groups at the end of the experiment. The average daily intake of minerals per mouse adjusted by the average dietary intake through the 6 mo of the experimental period is presented in Table 3. The addition of approximately 3% fish powder to the Ca-deficient purified diet provided the FC group with a 22% higher food intake than the CT group, which led to overall increases in mineral intake. Increases in Si intakes were observed as 253-fold in the Si group, 2.5-fold in the CS and FC groups, and 1.5-fold in the FSC group as compared with the control, respectively. The Si intake of the Si group was quite high compared with other groups, but its limited portion might have been absorbed by the gastrointestinal tract because the conversion rate of sodium metasilicate added to the diet as monomeric silicic acid, i.e., soluble silica, is unknown.

In bone biochemical properties, femoral dry and ash weights significantly increased in the Si group and ash weight in the FSC group (Fig. 1A). Femoral Ca contents increased significantly in the Si and CS groups and decreased in the FC group (Fig. 1B). The activities of tibial ALP, a marker of bone formation, increased significantly from 13% to 31% in all test groups except the EC group (Fig. 1C), indicating stimulatory effects on bone formation by Si intake as presented in Table 3. The prominent suppression of TRACP activity, a marker of bone resorption, was observed at 28% in the Si group and 18% in the CS group, whereas 31% activation was observed in the FC group (Fig. 1C). Femoral collagen content, determined as OHPro, increased significantly from 6% to 11% in the Si, CS, and FSC groups (Fig. 2A), whereas urinary excretion was suppressed to 8% in the Si group and 21% in the FSC group (Fig. 2B), indicating the suppression of bone resorption. In contrast, a significant 25% increase of urinary OHPro excretion was observed in the FC group. In bone mechanical properties, compared with the control, the Si group increased and the FC group decreased the strength of bone and the structural stiffness significantly, whereas the

Table 3
Daily intake of minerals per mouse*

Groups	CT	Si	CS	FCS	FC	EC
Diet intake (g)	6.78 ± 0.73 (100)	6.46 ± 0.81 (95)	6.66 ± 1.35 (98)	7.14 ± 1.3 (108)	8.04 ± 1.7† (122)	7.06 ± 0.9 (107)
Ca (mg)	49.64 ± 5.46 (100)	47.31 ± 6.15 (95)	48.83 ± 9.77 (98)	53.77 ± 9.78 (108)	60.54 ± 12.37† (122)	53.15 ± 6.93 (107)
Mg	10.44 ± 1.15 (100)	9.95 ± 1.29 (95)	13.28 ± 2.66† (130)	11.90 ± 2.16 (114)	13.70 ± 2.80† (131)	11.16 ± 1.45 (107)
Na	10.44 ± 1.15 (100)	9.95 ± 1.29 (95)	10.66 ± 2.13 (105)	11.31 ± 2.06 (108)	12.74 ± 2.60† (122)	11.16 ± 1.45 (107)
K	37.83 ± 4.16 (100)	36.05 ± 4.69 (95)	37.14 ± 7.43 (101)	40.94 ± 7.45 (108)	46.07 ± 9.41† (122)	40.44 ± 5.27 (107)
P	36.09 ± 3.97 (100)	34.40 ± 4.47 (95)	35.41 ± 7.08 (98)	39.05 ± 7.11 (108)	73.42 ± 15.00† (203)	38.58 ± 5.03 (107)
Fe (mg)	1.431 ± 0.157 (100)	1.364 ± 0.177 (95)	1.417 ± 0.283 (102)	1.565 ± 0.285 (109)	1.694 ± 0.346† (118)	1.488 ± 0.194 (104)
Zn	0.222 ± 0.024 (100)	0.211 ± 0.027 (98)	0.218 ± 0.044 (101)	0.237 ± 0.044 (107)	0.270 ± 0.055† (122)	0.237 ± 0.031 (107)
Cu	0.033 ± 0.004 (100)	0.031 ± 0.004 (98)	0.032 ± 0.006 (102)	0.035 ± 0.006 (106)	0.040 ± 0.008† (122)	0.035 ± 0.005 (107)
Mn	0.238 ± 0.026 (100)	0.227 ± 0.029 (98)	0.249 ± 0.050 (111)	0.254 ± 0.048 (107)	0.290 ± 0.058† (122)	0.254 ± 0.032 (107)
Si (μg)	0.84 ± 0.09 (100)	213.10 ± 27.70† (25 263)	2.12 ± 0.43† (252)	1.26 ± 0.23† (149)	2.17 ± 0.44† (257)	0.94 ± 0.12† (112)

Ca, calcium; CS, coral sand; CT, calcium carbonate (control); Cu, copper; EC, eggshell; FC, fish bone; Fe, iron; FSC, fossil stony coral; K, potassium; Mg, magnesium; Mn, manganese; Na, sodium; P, phosphorus; Si, silicon; Zn, zinc

* Values are means ± SDs for 10 mice each (percentages).

† $P < 0.05$ versus CT.

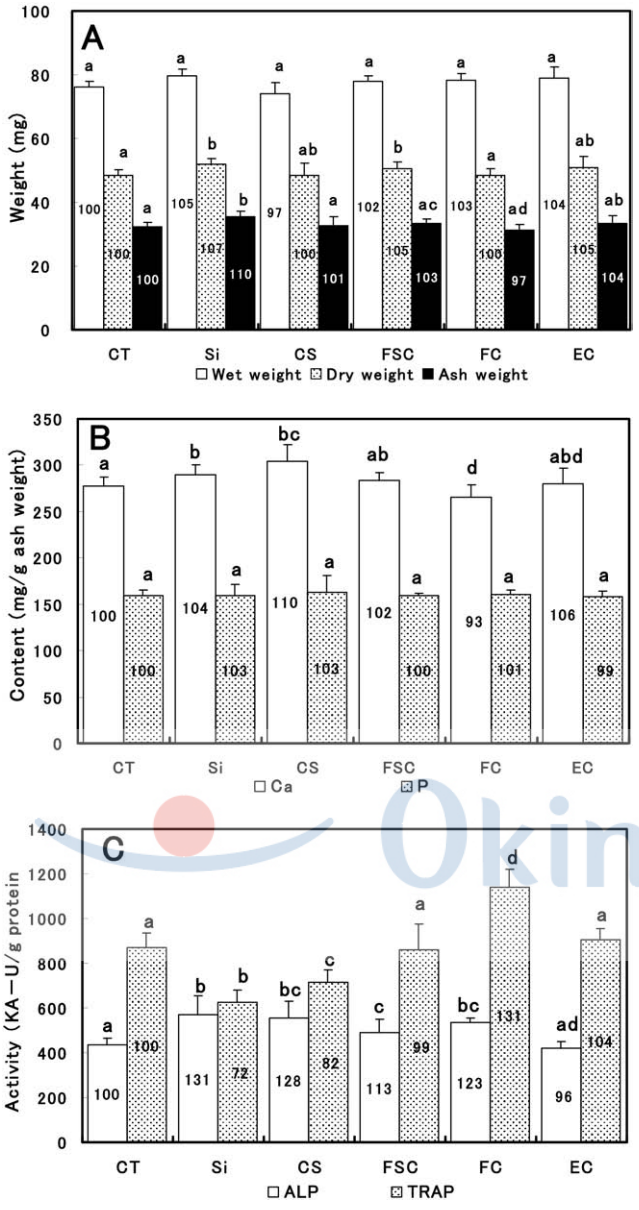

Fig. 1. Effects on femoral weights (A), Ca and P contents (B), and tibial ALP and TRACP activities (C). Values are means ± SDs for 10 animals in each group. Means with a different letter are significantly different at $P < 0.05$ (Duncan's new multiple range test). Diets are described in MATERIALS AND METHODS. ALP, alkaline phosphatase; Ca, calcium; CS, coral sand; CT, calcium carbonate (control); EC, eggshell; FC, fish bone; FSC, fossil stony coral; P, phosphorus; Si, silicon; TRACP, tartrate-resistant acid phosphatase.

FSC group significantly increased the amount of energy absorbed before breaking in mouse femurs (Fig. 3).

Effects on gene expression related to osteoblastogenesis and osteoclastogenesis

Changes in the gene expression of bone formation- and resorption-specific markers are summarized in Figure 4. The mRNA expressions related to osteoblastogenesis (Fig. 4A–E) significantly increased 44% and 33% in the Si and CS groups for Runx2 (Fig. 4A), 26% in the FSC group for IL-11 (Fig. 4C), and 19% and 34% in the Si and CS groups for COL1A1 (Fig. 4D), respectively, compared with the $CaCO_3$ control group, whereas the expressions significantly decreased 23% in the FC group for Runx2, 24% in the EC group for IL-11, and 17% and 39% in the FSC and EC groups for COL1A1, respectively. In contrast, PPAR-γ expression (Fig. 4E) significantly decreased 54%, 50%, and 24% in the Si, CS, and FSC groups, respectively, whereas it significantly increased 24% and 19% in the FC and EC groups, respectively. In the mRNA expression related to osteoclastogenesis (Fig. 4F–I), TGF-β (Fig. 4F) significantly decreased 25% and 31% in the Si and CS groups, respectively. There was a significant decrease in OPG observed only in the EC group, whereas RANKL significantly decreased 50% and 16% in the Si and CS groups, respectively, and increased 26% in the EC group. When the ratio of OPG to RANKL was taken, 94% and 21% greater expressions of OPG than RANKL were observed in the Si and CS groups, respectively, whereas 26% and 41% lower expressions were found in the FC and EC groups, respectively, as compared with the control (Fig. 4G).

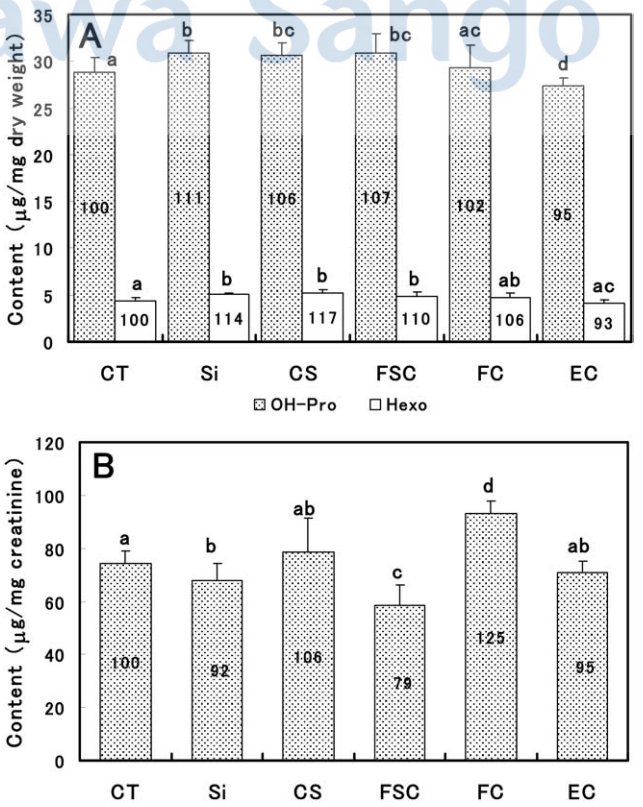

Fig. 2. Effects on femoral OH Pro content (A) and its urinary excretion (B). Values are means ± SDs. Means with a different letter are significantly different at $P < 0.05$. CS, coral sand; CT, calcium carbonate (control); EC, eggshell; FC, fish bone; FSC, fossil stony coral; Hexo, hexosamines; OH Pro, hydroxyproline; Si, silicon.

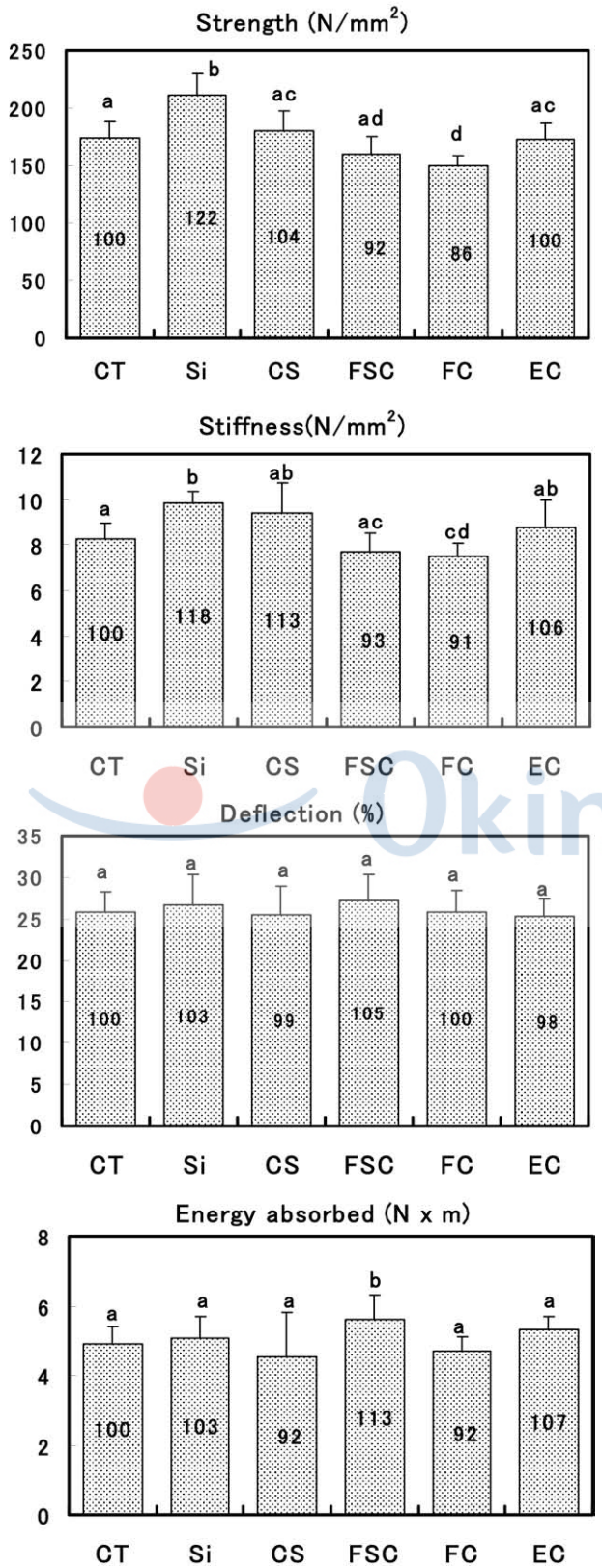

Fig. 3. Effects on mechanical properties of the femurs. Values are means ± SDs. Means with a different letter are significantly different at $P < 0.05$. CS, coral sand; CT, calcium carbonate (control); EC, eggshell; FC, fish bone; FSC, fossil stony coral; Si, silicon.

Discussion

In the present study of bone biochemical properties (Figs. 1 and 2), the Si, CS, and FSC groups in order of soluble Si intake (Table 3) showed a significant increase of bone ALP activity and significant suppressions of TRAP activity and urinary excretion of OHPro together with increases in bone Ca, OHPro, and Hex contents, suggesting the stimulation of bone mineralization. In contrast, the FC group showed significant increases of TRAP activity and urinary excretion of OHPro together with a decrease in bone Ca content, suggesting stimulation of resorptive bone turnover. In bone mechanical properties (Fig. 3), compared with the $CaCO_3$ control, the Si group and the CS group, to a lesser extent, exhibited improved mechanical properties of bone: increases in the strength and stiffness of femurs from SAMR1. Conversely, the FC group showed significant decreases of strength and stiffness, reflecting the bone biochemical properties observed. The FC group, despite its high Si intake (Table 3), showed the worst effects on biochemical and mechanical properties of bone, probably due to its high phosphorus intake (Table 3), as reported by excessive intake of phosphorus in humans [26,27] and in laboratory animals [6].

In addition to the biochemical and biomechanical changes observed, the mRNA expressions of related genes were studied. Runx2, also known as Cbfa1, is a master transcriptional factor for osteoblast differentiation during bone formation [28]. Runx2-binding sites are found in the promoters of osteoblastogenetic marker genes, including ALP, COL1A1, osteopontin, RANKL, and osteocalcin [28]. Runx2 is a downstream target of TGF-β and BMP-2, mediating the inhibitory effect of these factors on myogenic differentiation of C2C12 pluripotent mesenchymal precursor cells [29]. The induction of osteoblast-specific gene expression in these cells requires co-ordinated action between Runx2 and BMP-2–induced Smad5 [30]. TGF-β stimulates proliferation and early osteoblast differentiation, inducing the expression of Runx2 in combination with BMP-2, while inhibiting terminal differentiation. Smad3, activated by TGF-β, physically interacts with Runx2 at Runx2-responsive elements, thus suppressing the expression of Runx2 and other osteogenic genes such as COL1A1, ALP, and osteocalcin [31]. TGF-β also opposes BMP-2–induced Runx2 expression [32], which is mediated by Dlx5, a bone-inducing transcription factor expressed in later stages of osteoblast differentiation, by the suppression of Dlx5 expression [33]. IL-11 alone and in combination with BMP-2 synergistically induces the osteoblastic differentiation of mouse mesenchymal progenitor cells [34], bone marrow stromal cell line, and bone marrow cells [35]. In the present study, significant stimulation of Runx2 expression was observed in the Si and CS groups without any changes in the expressions of BMP-2 and IL-11 (Fig. 4A–C), but with significant suppressions of TGF-β (Fig. 4F). The observed increases of Runx2 expression in the two groups may

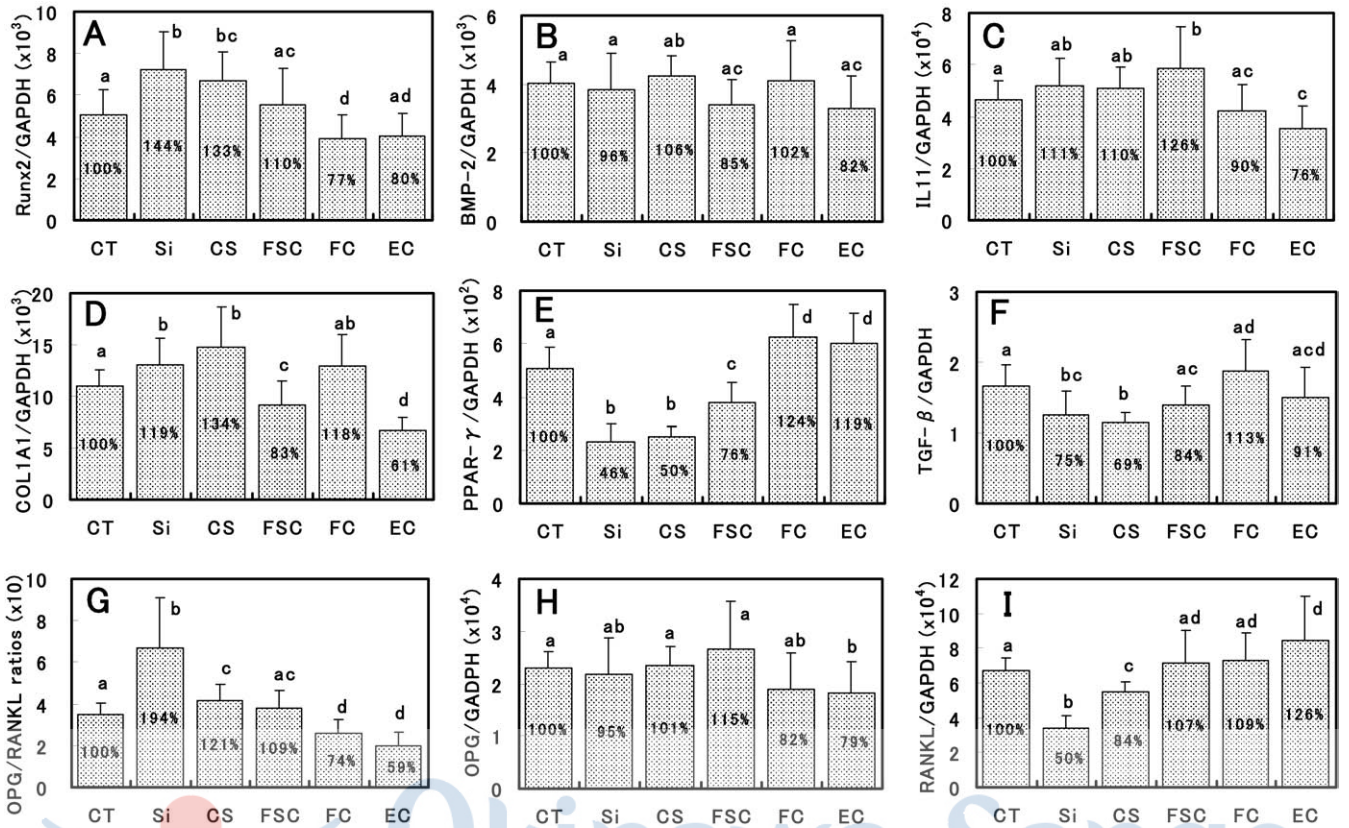

Fig. 4. Effects on the expression of mRNA related to osteoblastogenesis (A: Runx2, B: BMP-2, C: IL-11, D: COL1A1, E: PPAR-γ) and osteoclastogenesis (F: TGF-β, G: OPG/RANKL ratio, H: OPG, I: RANKL). Values are means ± SDs. Means with a different letter are significantly different at $P < 0.05$. BMP-2, bone morphogenic protein-2; COL1A1, type I procollagen; CS, coral sand; CT, calcium carbonate (control); EC, eggshell; FC, fish bone; FSC, fossil stony coral; GAPDH, glyceraldehydes-3-phosphate dehydrogenase; IL-11, interleukin-11; OPG, osteoprotegerin; PPAR-γ, peroxisome proliferator-activated receptor-γ; RANKL, receptor activator of nuclear factor-κB ligand; Runx2, runt-related transcription factor-2; Si, silicon; TGF-β, transforming growth factor-β.

be partly derived from suppression of the inhibitory effect of TGF-β on the expression of Runx2 and other osteogenic genes, as seen in the increased expression of COL1A1 (Fig. 4D) and ALP activity (Fig. 1C).

Peroxisome proliferator-activated receptor-γ, a ligand-activated transcription factor and a member of the nuclear hormone receptor superfamily, is expressed predominantly in adipose tissue and plays a critical role in the regulation of adipocyte differentiation [36,37]. Adipocytes and osteoblasts share a common pluripotent mesenchymal precursor [38,39]. Overexpression or activation of PPAR-γ induces adipogenesis over osteoblastogenesis in pluripotent cells [40,41], whereas PPAR-γ insufficiency enhances osteogenesis through osteoblast formation from bone marrow progenitors [42]. Adipocytic proportion of bone marrow is inversely related to bone formation in aging [43] and osteoporosis [44]. Cumulative evidence also indicates that thiazolidinediones, antidiabetic agents, and potent PPAR-γ agonists increase adipogenesis at the expense of osteogenesis, leading to bone loss [45,46]. In the present study, compared with the $CaCO_3$ control group, prominent suppression of PPAR-γ expression (Fig. 4E) was observed 54%, 50%, and 24% in the Si, CS, and FSC groups, respectively, leading to stimulation of bone formation, as exhibited by increases in bone dry and ash weights, femoral Ca contents, and the activities of tibial ALP (Fig. 1). In contrast, significant activations of 24% and 19% were obtained in the FC and EC groups, respectively, leading to stimulation of bone resorption, as exhibited by the suppression of Runx2 expression (Fig. 4A), decreased femoral Ca contents (Fig. 1B), and decreases of femoral strength and stiffness in the FC group (Fig. 3).

Osteoclasts are bone-resorbing multinucleated cells derived from hematopoietic progenitor cells of monocyte–macrophage lineage [47]. Osteoblasts/stromal cells play an essential role in osteoclastogenesis at bone-resorbing sites under the control of osteotropic hormones and local factors produced in the microenvironment by expressing a specific receptor activator of the nuclear factor-κB ligand (RANKL)/osteoclast differentiation factor/osteoprotegerin ligand/tumor necrosis factor-related activation-induced cytokine on their cell surface [47]. A multifunctional cytokine TGF-β, which is abundant in bone matrix, is involved not only in osteoblast differentiation, as discussed above, but also in osteoclast differentiation [48,49]. Direct effects of TGF-β on osteoclast precursors, such as upregulation of RANK expression

and induction of nuclear factor-κB activation, are responsible for this stimulatory effect on osteoclast differentiation. Transgenic mice overexpressing TGF-β_2 exhibited an osteoporosis-like phenotype due to increased osteoclastic function [50], and transgenic mice expressing dominant negative type II TGF-β receptor showed decreased osteoclastic bone resorption [51]. The suppression of TGF-β expression in the Si, CS, and FSC groups in this study (Fig. 4F) impairs osteoclast formation, as found in the decreased TRACP activity in those groups (Fig. 1C) and thus decreased bone resorption, together with suppression of the inhibitory effect of TGF-β on the expression of Runx2 and other osteogenic genes, as discussed above. Alternatively, increased expression of TGF-β in the FC group may be related to the prominent activation of TRACP (Fig. 1C).

Osteoblasts/stromal cells also produce OPG/osteoclastogenesis inhibitory factor, a soluble decoy receptor for RANKL, which inhibits the differentiation and activation of osteoclasts [47]. Regulation of the balance between the gene expressions of those two factors, RANKL and OPG, produced by osteoblasts in the bone microenvironment, is important for osteoclast development, and various osteotropic agents are involved in the regulatory mechanisms [52]. The expression of RANKL in this study was suppressed markedly in the Si group and next in the CS group in order of soluble Si intake, whereas there were no distinct alterations in the OPG expression in the Si, CS, and FSC groups but suppression was observed in the FC and EC groups. Consequently, the ratio of OPG mRNA to RANKL mRNA compared with the control was increased in the Si and CS groups but was below the control in the FC and EC groups (Fig. 4G–H). These changes were associated with decreased osteoclast formation in the Si and CS groups and with stimulated induction of osteoclastogenesis in the FC and EC groups. Although the mechanism underlying the suppression of RANKL is unknown in the present study, it is likely derived from the Si content in the diet compared with the $CaCO_3$ control diet. Taken together, the present study indicated that consideration of coexisting bone-seeking trace elements in Ca sources for its supplementation is an important factor. The mechanisms behind the beneficial effects of Si on bone remodeling need to be further clarified, from the nutritional viewpoint, to prevent and improve osteoporosis.

Conclusion

In conclusion, the effects of Si on biochemical and biomechanical properties of bone and gene expression associated with bone remodeling in the present study strongly suggest that soluble Si contributes to bone quality through the dual action of stimulating bone formation and inhibiting bone resorption.

References

[1] Parfitt AM, Villanueva AR, Foldes J, Rao DS. Relations between histologic indices of bone formation: Implications for the pathogenesis of spinal osteoporosis. J Bone Miner Res 1995;10:466–73.
[2] National Osteoporosis Foundation. America's bone health: the state of osteoporosis and low bone mass. Washington, DC: National Osteoporosis Foundation; 2004. Available at: http://www.nof.org/advocacy/prevalence/index.htm. Accessed March 1, 2008.
[3] O'Fraherty EJ. Modeling bone mineral metabolism, with special reference to calcium and lead. Neurotoxicology 1992;13:789–97.
[4] Brown EM, MacLeod JR. Extracellular calcium sensing and extracellular calcium signaling. Physiol Rev 2001;81:239–97.
[5] Zaidi M, Shankar VS, Tunwell R, Adebanjo OA, McKrill J, Pazianas M, et al. A ryanodine receptor-like molecule expressed in the osteoclast plasma membrane functions in extracellular Ca^{2+} sensing. J Clin Invest 1995;96:1582–90.
[6] Brown AJ, Ritter CS, Finch JL, Slatopolsky EA. Decreased calcium-sensing receptor expression in hyperplastic parathyroid glands of uremic rats: role of dietary phosphate. Kidney Int 1999;55:1284–92.
[7] Dahl SG, Allain P, Marie PJ, Mauras Y, Boivin G, Ammann P, et al. Incorporation and distribution of strontium in bone. Bone 2001;28:446–53.
[8] Quarles DL, Hartle JE, Siddhanti SR, Guo R, Hinson TK. A distinct cation-sensing mechanism in MC3T3-E1 osteoblasts functionally related to the calcium receptor. J Bone Miner Res 1997;12:393–402.
[9] Saltman PD, Strause LG. The role of trace minerals in osteoporosis. J Am Coll Nutr 1993;12:384–9.
[10] Carlisle EM. Silicon: an essential element for the chick. Science 1972;178:619–21.
[11] Schwarz K, Milne DB. Growth-promoting effects of silicon in rats. Nature 1972;239:333–4.
[12] Carlisle EM. Silicon: a possible factor in bone calcification. Science 1970;167:279–80.
[13] Carlisle EM. Silicon. In: Frieden E, editor. Biochemistry of the essential ultratrace elements. New York: Plenum Press; 1984, p. 257–91.
[14] Perry CC, Keeling-Tucker T. Aspects of bioinorganic chemistry of silicon in conjunction with the biometals calcium iron and aluminium. J Inorg Biochem 1998;69:181–91.
[15] Poppwell JF, King SJ, Day JP, Ackrill P, Fifield LK, Cresswell RG, et al. Kinetics of uptake and elimination of silicic acid by a human subject: a novel application of 32Si and accelerator mass spectrometry. J Inorg Biochem 1998;69:177–80.
[16] Reffitt DM, Jugdaohsingh R, Thompson RPH, Powell JJ. Silicic acid: its gastrointestinal uptake and urinary excretion in man and effects on aluminium excretion. J Inorg Biochem 1999;76:141–7.
[17] LeVier RR. Distribution of silicon in the adult rat and rhesus monkey. Bioinorg Chem 1975;4:109–15.
[18] Maehira F, Iinuma Y, Eguchi Y, Miyagi I, Teruya S. Effects of soluble silicon compound and deep-sea water on biochemical and mechanical properties of bone and the related gene expression in mice. J Bone Miner Metab 2008;26:446–55.
[19] Tarutani T. Polymerization of silicic acid. Anal Sci 1989;5:245–52.
[20] Podenphant J, Larsen N-E, Christiansen C. An easy and reliable method for determination of urinary hydroxyproline. Clin Chim Acta 1984;142:145–8.
[21] Nakamura T, Kurokawa T, Orimo H. Increased mechanical strength of the vitamin D-replete rat femur by the treatment with a large dose of 24R, $25(OH)_2D_3$. Bone 1989;10:117–23.
[22] Taussky HH, Shorr E. A microcolorimetric method for the determination of inorganic phosphorus. J Biol Chem 1953;202:675–85.
[23] Woessner JF Jr. The determination of hydroxyproline in tissue and protein samples containing small proportions of this amino acid. Arch Biochem Biophys 1961;93:440–7.

[24] Carlisle EM. Biochemical and morphological changes associated with long bone abnormalities in silicon deficiency. J Nutr 1980;110: 1046–55.
[25] Good TA, Bessman SP. Determination of glucosamine and galactosamine using borate buffers for modification of the Elson-Morgan and Morgan-Elson reactions. Anal Biochem 1964;9:253–62.
[26] Wyshak G, Frisch RE. Carbonated beverages, dietary calcium, the dietary calcium/phosphorus ratio, and bone fractures in girls and boys. J Adolesc Health 1994;15:210–5.
[27] Calvo MS, Kumar R, Heath H. Persistently elevated parathyroid hormones secretion and action in young women after four weeks of ingesting high phosphorus, low calcium diets. J Clin Endocrinol Metab 1990;70:1334–40.
[28] Stein GS, Lian JB, van Wijnen AJ, Stein JL, Montecino M, Javed A, et al. Runx2 control of organization, assembly and activity of the regulatory machinery for skeletal gene expression. Oncogene 2004; 23:4315–29.
[29] Lee MH, Javed A, Kim HJ, Shin HI, Gutierrez S, Choi JY, et al. Transient upregulation of CBFA1 in response to bone morphogenetic protein-2 and transforming growth factor β1 in C2C12 myogenic cells coincides with suppression of the myogenic phenotype but is not sufficient for osteoblast differentiation. J Cell Biochem 1999;73:114–25.
[30] Lee KS, Kim HJ, Li QL, Chi XZ, Ueta C, Komori T, et al. Runx2 is a common target of transforming growth factor β1 and bone morphogenic protein 2, and cooperation between Runx2 and Smad5 induces osteoblast-specific gene expression in the pluripotent mesenchymal precursor cell line C2C12. Mol Cell Biol 2000;20:8783–92.
[31] Alliston T, Choy L, Ducy P, Karsenty G, Derynck R. TGF-β–induced repression of CBFA1 by Smad3 decreases cbfa1 and osteocalcin expression and inhibits osteoblast differentiation. EMBO J 2001;20: 2254–72.
[32] Spinella-Jaegle S, Roman-Roman S, Faucheu C, Dunn FW, Kawai S, Gallea S, et al. Opposite effects of bone morphogenetic protein-2 and transforming growth factor-β1 on osteoblast differentiation. Bone 2001;29:323–30.
[33] Lee MH, Kim YJ, Kim HJ, Park HD, Kang AR, Kyung HM, et al. BMP-2–induced Runx2 expression is mediated by Dlx5, and TGF-β1 opposes the BMP-2–induced osteoblast differentiation by suppression of Dlx5 expression. J Biol Chem 2003;278:34387–94.
[34] Suga K, Saitoh M, Fukushima S, Takahashi K, Nara H, Yasuda S, Miyata K. Interleukin-11 induces osteoblast differentiation and acts synergistically with bone morphogenic protein-2 in C3H10T1/2 cells. J Interferon Cytokine Res 2001;21:659–707.
[35] Takeuchi Y, Watanabe S, Ishii G, Takeda S, Nakayama K, Fukumoto S, et al. Interleukin-11 as a stimulatory factor for bone formation prevents bone loss with advancing age in mice. J Biol Chem 2002; 277:49011–8.
[36] Spiegelman BM, Flier JS. Adipogenesis and obesity: rounding out the big picture. Cell 1996;87:377–89.
[37] Rosen ED, Spiegelman BM. PPAR-γ: a nuclear regulator of metabolism, differentiation, and cell growth. J Biol Chem 2001;276: 37731–4.
[38] Benett JH, Joyner CJ, Triffitt JT, Owen ME. Adipocytic cells cultured from marrow have osteogenic potential. J Cell Sci 1991;99:131–9.
[39] Pittenger MF, Mackay AM, Beck SC, Jaiswal RK, Douglas R, Mosca JD, et al. Multilineage potential of adult human mesenchymal stem cells. Science 1999;284:143–7.
[40] Lecka-Czernick B, Gubrij I, Moerman EJ, Kajkenova O, Lipschitz DA, Manolagas SC, Jilka RL. Inhibition of OSF2/Cbfa1 expression and terminal osteoblast differentiation by PPAR-γ2. J Cell Biochem 1999;74:357–71.
[41] Jeon MJ, Kim JA, Kwon SH, Kim SW, Park KS, Park SW, et al. Activation of peroxisome proliferator-activated receptor-γ inhibits the Runx2-mediated transcription of osteocalcin in osteoblasts. J Biol Chem 2003;278:23270–7.
[42] Akune T, Ohba S, Kamekura S, Yamaguchi M, Chung U, Kubota N, et al. PPAR-γ insufficiency enhances osteogenesis through osteoblast formation from bone marrow progenitors. J Clin Invest 2004;113: 846–55.
[43] Moerman EJ, Teng K, Lipschitz DA, Lecka-Czernick B. Aging activates adipogenic and suppresses osteogenic programs in mesenchymal marrow stroma/stem cells: the role of PPAR-γ2 transcription factor and TGF-β/BMP signal pathway. Aging Cell 2004;3:379–89.
[44] Verma S, Rajaratnam JH, Denton J, Hoyland JA, Byers RJ. Adipocytic proportion of bone marrow is inversely related to bone formation in osteoporosis. J Clin Pathol 2002;55:693–8.
[45] Ali AA, Weinstein RS, Stewart SA, Parfit AM, Manolagas SC, Jilka RL. Rosiglitazone causes bone loss in mice by suppressing osteoblast differentiation and bone formation. Endocrinology 2005;146: 1226–35.
[46] Li M, Pan LC, Simmons HA, Li Y, Healy DR, Robinson BS, et al. Surface-specific effects of a PPAR-γ agonist, darglitazone, on bone in mice. Bone 2006;39:796–806.
[47] Suda T, Takahashi N, Udagawa N, Jimi E, Gillespie MT, Martin TJ. Modulation of osteoclast differentiation and function by the new members of the tumor necrosis factor receptor and ligand families. Endocr Rev 1999;20:345–57.
[48] Kaneda T, Nojima T, Nakagawa M, Ogasawara A, Kaneko H, Sato T, et al. Endogenous production of TGF-β is essential for osteoclastogenesis induced by a combination of receptor activator of NF-κB ligand and macrophage-colony-stimulating factor. J Immunol 2000; 165:4254–63.
[49] Itonaga I, Sabokbar A, Sun SG, Kudo O, Danks L, Ferguson D. Transforming growth factor-β induces osteoclast formation in the absence of RANKL. Bone 2004;34:57–64.
[50] Erlebacher A, Derynck R. Increased expression of TGF-β2 in osteoblasts results in an osteoporosis-like phenotype. J Cell Biol 1996;132: 195–210.
[51] Filvaroff E, Erlebacher A, Ye JQ, Gitelman SE, Lotz J, Heillman M, et al. Inhibition of TGF-β receptor signaling in osteoblasts leads to decreased bone remodeling and increased trabecular bone mass. Development 1999;126:4267–79.
[52] Horwood NJ, Elliott J, Martin TJ, Gillespie MT. Osteotropic agents regulate the expression of osteoclast differentiation factor and osteoprotegerin in osteoblastic stomal cells. Endocrinology 1998;139: 4743–6.